

## Initial infrasound source characterization using the phase and amplitude gradient estimator method

Francisco J. Irrazabal, Mylan R. Cook, Kent L. Gee, Pauline Nelson, Daniel J. Novakovich, and Scott D. Sommerfeldt

Citation: *Proc. Mtgs. Acoust.* **36**, 045004 (2019); doi: 10.1121/2.0001097

View online: <https://doi.org/10.1121/2.0001097>

View Table of Contents: <https://asa.scitation.org/toc/pma/36/1>

Published by the [Acoustical Society of America](#)

---

### ARTICLES YOU MAY BE INTERESTED IN

[Synergy of spectral and spatial segregation cues in simulated cocktail party listening](#)

*Proceedings of Meetings on Acoustics* **36**, 050005 (2019); <https://doi.org/10.1121/2.0001092>

[Predicting pressure sensitivity through ontogeny in larval red drum \(\*Sciaenops ocellatus\*\)](#)

*Proceedings of Meetings on Acoustics* **37**, 010006 (2019); <https://doi.org/10.1121/2.0001098>

[A cross-linguistic comparison on the use of prosodic cues for ambiguity resolution](#)

*Proceedings of Meetings on Acoustics* **36**, 060005 (2019); <https://doi.org/10.1121/2.0001094>

[Infrasound emissions from tornadoes and severe storms compared to potential tornadic generation mechanisms](#)

*Proceedings of Meetings on Acoustics* **36**, 045005 (2019); <https://doi.org/10.1121/2.0001099>

[How POMA and other conference proceedings empower students to publish](#)

*Proceedings of Meetings on Acoustics* **36**, 032001 (2019); <https://doi.org/10.1121/2.0001001>

[Classifying crowd behavior at collegiate basketball games using acoustic data](#)

*Proceedings of Meetings on Acoustics* **35**, 055006 (2018); <https://doi.org/10.1121/2.0001061>

---



**POMA** Proceedings  
of Meetings  
on Acoustics

**Turn Your ASA Presentations  
and Posters into Published Papers!**



---

## 177th Meeting of the Acoustical Society of America

Louisville, Kentucky

13-17 May 2019

### Physical Acoustics: Paper 4aPA10

---

# Initial infrasound source characterization using the phase and amplitude gradient estimator method

**Francisco J. Irarrazabal, Mylan R. Cook and Kent L. Gee**

*Department of Physics and Astronomy, Brigham Young University, Provo, UT, 84602;  
firrazabal@gmail.com; mylan.cook@gmail.com, kentgee@byu.edu*

**Pauline Nelson**

*Department of Physics, Brigham Young University-Idaho, Rexburg, Rexburg, ID; pauline3white@gmail.com*

**Daniel J. Novakovich and Scott D. Sommerfeldt**

*Department of Physics and Astronomy, Brigham Young University, Provo, UT, 84602;  
danielnovakovich@gmail.com; scott\_sommerfeldt@byu.edu*

The phase and amplitude gradient estimator (PAGE) method for vector acoustic intensity [D.C. Thomas et al. *J. Acoust. Soc. Am.* 137, 3366–3376 (2015)] has been used previously to improve source characterization over broad frequency ranges. This paper describes the applications of the PAGE method in two outdoor infrasound sources characterization using multi-microphone probes. Measurements were made with a setup designed to address the challenges when dealing with outdoor infrasound sources, such as low coherence, noise contamination and microphone mismatch. Also, applying the acoustic intensity methods brings up analysis challenges including phase unwrapping above the spatial Nyquist frequency, source statistical stationarity, and balancing frequency resolution with averaging across finite record lengths. This paper describes the results of source characterization for a large rocket motor and a wind turbine using two different microphone probe setups, and how these measurement and analysis challenges performed with the probes setups.

## 1. INTRODUCTION

The acoustic intensity measurement method is widely used for source characterization and sound power estimation<sup>1</sup>. The active intensity is the time-averaged product of the particle velocity and the pressure and allows for vector mapping of acoustic energy flow. Despite relatively standard use in the audio range, intensity measurements in the infrasound region are rare and possibly nonexistent. This paper describes the application of a pressure-based intensity method to benchmark experiments involving two infrasound sources: a large solid-fuel rocket booster motor and a wind turbine. These initial results show that vector intensity is a promising method for obtaining frequency-dependent source locations at, and above, the infrasound regime.

The pressure-based method for vector intensity uses an array of microphones and then utilizes finite sums and differences of the pressures between microphones to obtain the requisite pressure and particle velocity. The connection between the finite pressure difference, i.e., the gradient, and the particle velocity is established by Euler's equation. Vector intensity measurements using a particle velocity sensor are also possible, but when flow is present, such as wind outdoors, these sensors are less robust than microphones<sup>2-4</sup>. The intensity calculation is then completed by the product between the averaged amplitude of the pressure and the estimated complex conjugate of the particle velocity. This method is well known and normally called the traditional p-p method.

Although likely more robust in outdoor environments, the pressure-based vector intensity method has limitations due to instrument amplitude and phase mismatch and bias errors due to the finite sums and differences when the sensor spacing is no longer small relative to a wavelength. The errors for these limitations are fairly well known<sup>5,6</sup> and addressing them gives a frequency band limit for accurate calculations. In the case of infrasound applications, microphone phase mismatch becomes a particular problem because of the rapid variation in relative phase between microphones near the microphone corner frequency. Having a large separation distance will cause the acoustic phase difference to be larger than the instrument mismatch, thus giving a better response for low frequencies, but this will lower the upper frequency limit of the probe. On the other hand, having a small separation distance will improve the accuracy of calculations for higher frequencies, but will reduce the instrument's accuracy at low frequencies. Thus, there is a frequency bandwidth limitation using the vector intensity method.

The phase and amplitude gradient estimator (PAGE) method for acoustic intensity<sup>7</sup> was developed to extend the usable frequency range of calculated intensity from multimicrophone probes, and has since been successfully applied to the audible and ultrasound range in different experiments<sup>8-10</sup>. This method uses dual-channel analysis quantities to express the spatial pressure field in terms of its amplitude and phase. Then, to calculate the acoustic intensity, instead of the particle velocity estimation this method uses both phase and amplitude gradients separately to compute the active and reactive intensity. This separation into magnitude and phase reduces bias errors and makes possible the extension of the useable frequency range of the probe. Because the PAGE method relies on transfer functions to estimate the phase gradient, phase unwrapping is possible, which increases the probe upper frequency limit. Furthermore, the reduced bias errors make possible larger microphone separation distances, which can improve the probe low-frequency limit that is caused by microphone or recording channel mismatch.<sup>11</sup>

The use of the PAGE method makes possible intensity measurements within the infrasound regime, while still allowing for the possibility of continued use within the audible regime. However, because regular on-the-market commercial intensity probes typically have a maximum microphone separation distance of 100 mm (limiting their use to above ~30 Hz), larger spacings must be used. This paper describes application of the PAGE method for infrasonic sources using free-field microphones with a larger separation distance than commercial intensity probes, but with a probe size that is relatively compact compared to state-of-the-art infrasonic arrays, where the normal separation distance between sensors can be on the order of hundreds of meters or even kilometers.<sup>12</sup>

The focus of this paper is the initial application of the PAGE method to the localization of two broadband sources with significant infrasound energy. Because these outdoor sources have essentially known directions, these are benchmark experiments to understand the strengths and limitations of the experimental setups. The next sections of this paper explain two experiments. For each experiment, the setup and conditions are described, after which the measurement results and the resulting acoustic intensity calculations are presented. Measurement challenges, such as microphone mismatch, wind and other noise sources, are discussed. Despite these challenges,

---

which point to important directions for future research results, the present results indicate a successful application of the PAGE method in the characterization of two different infrasound sources.

## 2. STATIC ROCKET MOTOR FIRING

Measurements were performed with two-dimensional vector intensity arrays using ½” free-field microphones. This experiment was conducted during a horizontal static firing of a large solid-fuel rocket motor and took place at the Northrop Grumman facilities in Promontory, Utah on the afternoon of the April 4 of 2019. The motor is a GEM 63 solid-fuel booster rocket motor with a graphite-epoxy casing type being developed for the Atlas V launch vehicle. It has 373,000 lbf of thrust with a burn time of 86 seconds.

### A. MEASUREMENT SETUP

The probe was located 1.6 km away from the source, at a location 57.5 degrees relative to the nozzle centerline. The measurement layout is shown in Figure 1. The path between the rocket nozzle and the microphone probe was surrounded by buildings and terrain bumps, this fact is believed to actually affect the sound propagation and the measured results. For this measurement, the probe consisted of four GRAS 46AE microphones that had been phase-matched as pairs above 30 Hz using the GRAS 51AB intensity calibrator. The microphones were arranged as an orthogonal probe as shown in Figure 2. The probe was mounted on a tripod, which was leveled and set at a height of 1.5 m off the ground. The microphones in each pair were separated by a distance of 0.5 m, resulting in a one-dimensional (1D) spatial Nyquist frequency of ~340 Hz. Each microphone was covered with a 90 mm diameter ball windscreen. Note that although these microphones were well phase matched above 30 Hz, based on the bandwidth of the intensity calibration, we had no information prior to this measurement regarding their phase matching below 30 Hz. Additionally, differing cutoff frequencies of the individual microphones (typically around ~3 Hz per the manufacturer specifications) means that the microphones’ relative phase response could possibly vary greatly within the infrasound region. Thus, this provides an opportunity to understand the suitability of using greater spacing to possibly extend the use of phase-matched microphone pairs within the infrasound regime.

The probe orientation was such that one microphone pair’s axis pointed to/away from the source and the other pair was perpendicular. The probe’s orientation was such that 0° corresponds to the expected sound intensity direction from the rocket. Although prior near-field intensity measurements of a similar GEM-60 rocket motor<sup>13</sup> described the extreme non-compactness and frequency dependence of the source, at this measurement distance, the source location can be considered compact, and frequency independent within 2°.

The propagation environment added to the test complexity. The probe was located a considerable distance from the source, with substantial terrain variation, multipath interference from scattering off buildings, and numerous spectators and vehicles in the vicinity of the probe, which was located about 20 m from a two-lane highway.

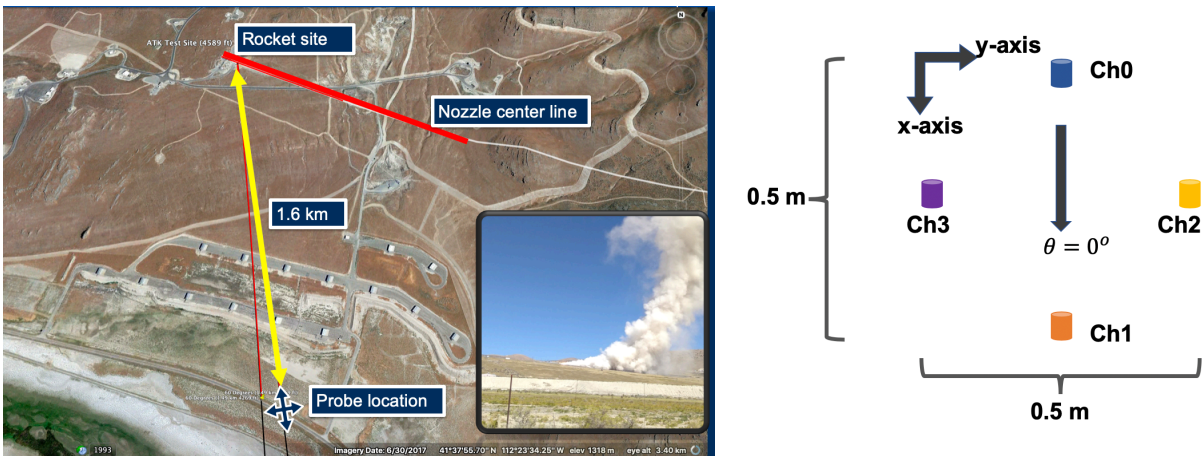


**Figure 1.** GEM-63 static measurement layout, with the probe at a distance of 1.6 km and the probe location was along the shoulder of a two-lane highway. The thick-red line shows the plume exhaust centerline. Left: Top view of the experiment setup, there were several buildings, terrain obstacles and people in the surroundings. Right: The coordinate axis was defined such that the positive X-axis pointed away from the sources (down in the picture).



**Figure 2.** Left: Intensity probe, with 0.5 m between orthogonal microphone pairs. Right: The probe location with the rocket test site in the upper part of the picture

## B. ROCKET MEASUREMENT RESULTS AND ANALYSIS

The results shown in this section are the autospectrum, the coherence, and the intensity direction and magnitude from the GEM-63 firing. A comparison between the autospectral sound pressure levels from the four microphones and the intensity level spectrum is a useful benchmark because, for propagating waves, the sound pressure level and the sound intensity level should be within 0.2 dB. Likewise, the known source location and probe orientation allows for the calculated intensity direction to be compared to the expected direction of  $0^\circ$ . Deviations from the expected results provide insights into measurement challenges and potential improvements.

The sound pressure level (autospectra) spectra from all four microphones are shown in Figure 3. The peak levels are found in the 7-50 Hz range, with a peak frequency of around 15-25 Hz. The spectral response from the microphones is extremely similar, but for frequencies below 2.5 Hz and above  $\sim 40$  Hz, some disagreement between the spectra is observed. In examining the coherence spectra in Figure 4, the coherence is close to one in the higher energy range (3 – 90 Hz, where the measured spectral levels are greater than 80 dB), but there is a noticeable drop in coherence in the frequencies where there is also spectral disagreement. The small differences in autospectra and the drop in coherence point to partial amplitude and phase randomization. The discrete frequency drops at around 60 and 80 Hz seem likely to be caused by different multipath interference effects, whereas the overall high-frequency drop in the coherence is likely due to ground reflections and atmospheric turbulence. Differences in low-frequency microphone response could also contribute to the spectral disagreement below 3 Hz (but would not impact the coherence).

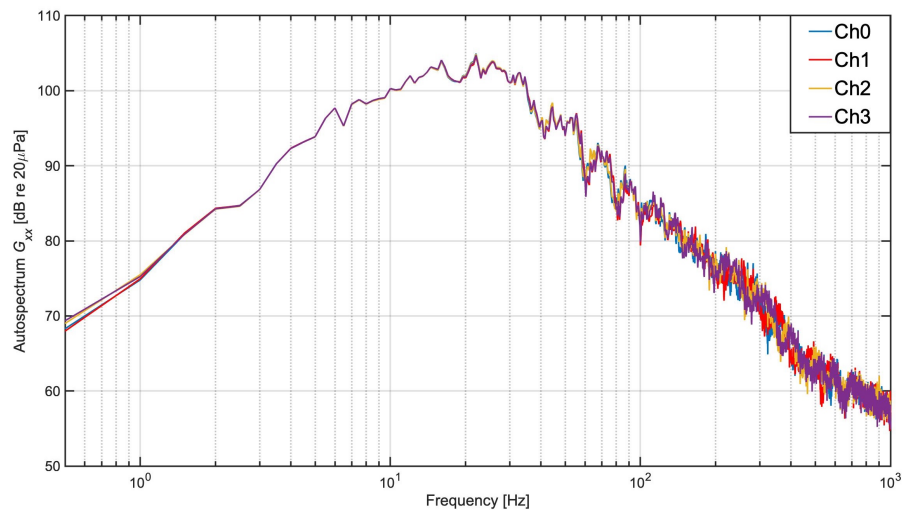


**Figure 3. Probe autospectra obtained from the rocket experiment.**

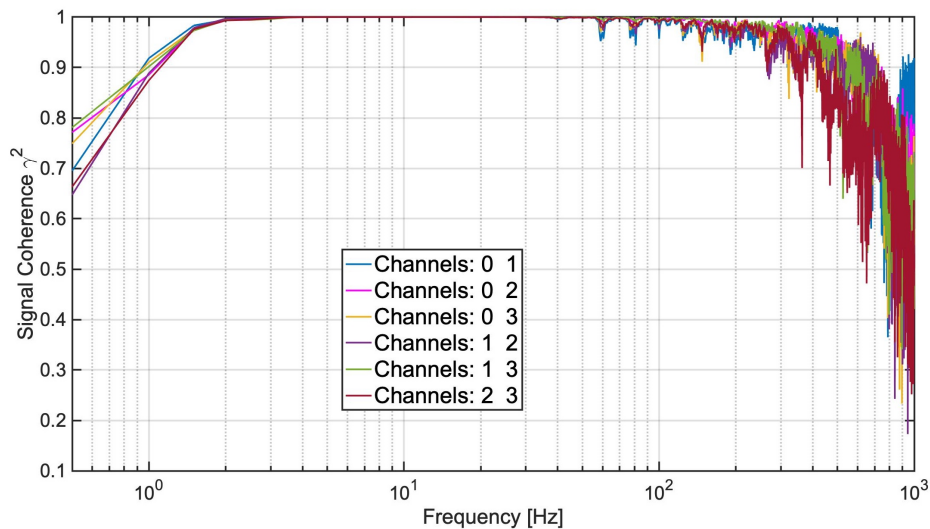


**Figure 4. Coherence between probe channels.**

The acoustic intensity magnitude estimation for the GEM-63 rocket firing is shown in Figure 5. The magnitude is well matched with the mean autospectrum between  $\sim 5$  Hz to the maximum analysis bandwidth for the PAGE method with phase unwrapping, and up to 200 Hz for the traditional p-p method. The limitations outlined in the Introduction are clearly noticeable here, since the errors for the traditional method become large as the spatial Nyquist frequency is approached. In the low-frequency region (below 2.5 Hz), there is also a large error that grows up to 15 dB. Because the mean autospectrum does not have significant evidence of wind noise, the most likely cause for these large errors in the intensity magnitude is instrumentation mismatch. The dips in both coherence and in mean autospectrum magnitude at  $\sim 0.5$  Hz suggests some sort of interference phenomenon.

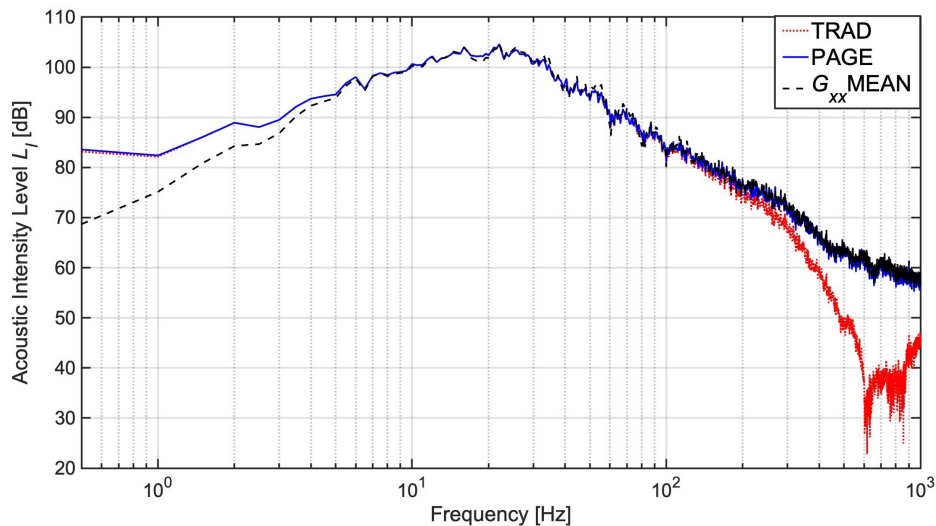


**Figure 5.** Acoustic intensity level as a function of frequency, benchmarked with the autospectrum for the propagating wave case.

The intensity direction calculated as a function of frequency is also informative. Figure 6 shows the results for both the traditional method and PAGE method, calculated with a 0.5 Hz resolution. The correct direction, according to the experimental setup, was near zero degrees. The intensity direction estimations from both methods match very well up to about 300 Hz, where the traditional method has a noticeable variation (caused by bias errors), followed by erratic behavior (due to spatial aliasing). Above approximately 5 Hz, the calculated direction from the PAGE method oscillates around a mean of near zero degrees, certainly within the precision of visually aligning the probe. However, below 5 Hz (approaching the microphones' cutoff frequency), large errors in direction calculation for both intensity methods appear. We believe this drift to be primarily caused by phase and amplitude mismatch between the microphones. Also apparent in Figure 6 are the effects of reflections that appear at regular intervals of  $\sim 20$  Hz, beginning at 40 Hz (and possibly even 20 Hz) that cause oscillations in the intensity direction. One possible cause is the buildings between the test site and the measurement location. Another is reflections off the spectators' vehicles to the rear of the probe. Overall, this experiment yielded a fair calculation for acoustic intensity magnitude and direction in the upper infrasound and low audio region. These are promising results for the microphones used (phase matched only at 30 Hz and above) and the probe configuration.

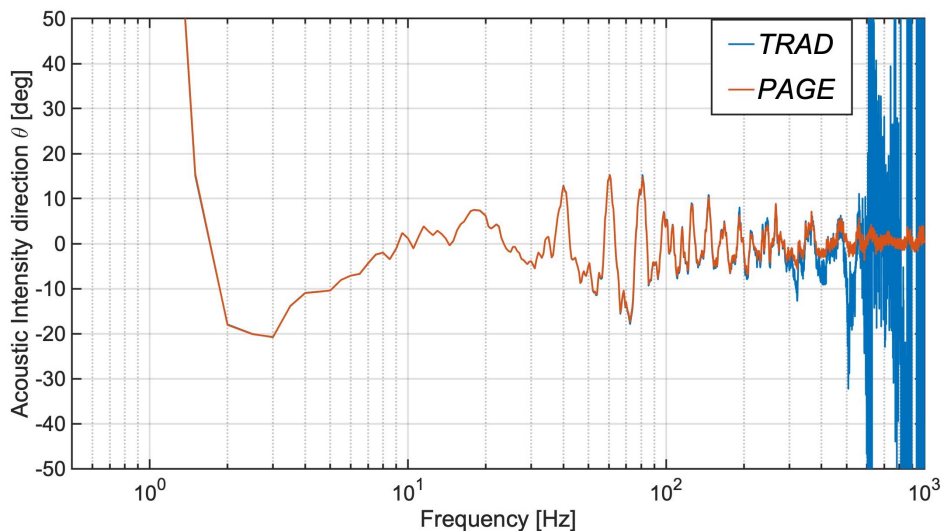


**Figure 6.** Calculated vector intensity direction as a function of frequency from the GEM-63 rocket, for both the traditional and PAGE methods.

This experiment yielded a fair calculation for acoustic intensity magnitude and direction in the upper infrasound and low audio region. These are promising results for the microphones used (phase matched only at 30 Hz and above) and the probe configuration.

### 3. WIND TURBINE EXPERIMENT

The second experiment is meant to show the application of the PAGE method to the acoustic measurement of a wind turbine, specifically for source localization and tonal noise separation. The measurement was performed at the Utah National Guard's Camp Williams during August of 2018, where there are two wind turbines in close proximity. Although data were collected with both turbines operating, for this paper, data collected with only one turbine spinning are analyzed. The turbine is a Vestas V47/660 with a 47 m rotor diameter, three blades with 22.9 m length and a rated power of 660 kW.

#### A. MEASUREMENT SETUP

The vector probe, located at a distance of 15 m from the base of the turbine, consisted of four microphones, three at the vertices of an equilateral triangle and one at the center. This center microphone is used to obtain the pressure amplitude. The distance between the center and each vertex was 3.0 m, with a distance of 5.30 m between each vertex, as shown in Figure 7. The microphones were inverted above a 16" diameter ground plate, covered by a reticulated foam windscreen. The microphones used in this configuration were PCB model 378A07, which are infrasound-capable down to 0.1 Hz (-2 dB). The phase characteristics of the microphones were unknown, and no phase calibration was performed. Phase calibration in the infrasound regime is left to future work.

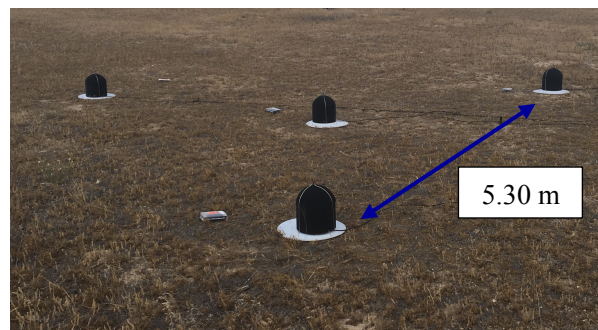


*Figure 7. Wind turbine intensity probe configuration.*

Although calibration of the microphones at these low frequencies has not been performed, the probe geometry is conducive to operation in the infrasound region. First, the relatively large inter-microphone distances increase the possibility of the acoustic phase difference being large relative to the electromechanical differences between channels. For this probe, the 1D spatial Nyquist frequency for the vertex-to-vertex spacing is approximately 32 Hz. Although the 2D arrangement increases this limit, a prior application<sup>14</sup> of this geometry to localization for an outdoor subwoofer showed that the traditional intensity method had a large jump in angle error at approximately 80 Hz, and erratic behavior below 8 Hz.

On the other hand, the distance between the microphones at the center and at each vertex is smaller than the distance between microphones at two vertices but this microphone at the center is giving the measured complex pressure instead of having an averaged from the vertex.

The location where the experiment was held is shown in Figure 8. The vector intensity probe was configured to be a distance of 15 m from the wind turbine, with the orientation such that one vertex pointed outward from the wind turbine. The x axis pointed from the center microphone to that vertex, such that the intensity from the turbine is expected to point in the direction of 0° for ideal conditions. However, factors that contributed to a nonideal environment include scattering of radiated sound by nearby military vehicles, wind noise, a large gravel-mining operation, and the I-15 highway, which though approximately 1.2 km away, was distinctly audible. The wind condition was measured by a Kestrel 5500 portable weather meter station, which when averaged over measurement period gave a wind speed of 2.3 m/s and a wind direction coming from the north east, which means a cross component through the probe as shown in Fig. 8. The gravel mining operation, which

is the most dominant contaminating noise source, was located at an approximate heading of  $90^\circ$  relative to the probe  $x$  axis. In summary, other noise sources were present which can affect the intensity calculations using the PAGE method.



**Figure 8.** Vestas V47/660 wind turbine experiment setup. The red asterisk shows the wind turbine location, and the triangle the probe location, the thin-gray line going downwards in the picture shows the zero degree axis. The approximate location of the gravel mining operation is also shown.

## B. WIND TURBINE EXPERIMENT RESULTS AND ANALYSIS

The analysis for the wind turbine experiment is focused on selected frequencies instead of a broadband analysis. This is because of the high noise coming from other sources, such that the broadband spectra and the intensity calculations are based on energy radiated by several sources. From the autospectra shown in Figure 9, it is possible to see the broadband components and peaks at certain frequencies coming from tonal sources. Also from Figure 9, the spectra are mostly flat above 50 – 200 Hz, with the peaks not much higher than the broadband level. Therefore, for this case the analysis focus will be below 45 Hz. The detailed autospectra for the 0-45 Hz frequency band is shown in Figure 10, where the peak components can be separated in three harmonic series with fundamentals of 1.9, 13.1 and 20 Hz. In addition, Figure 10 uses a linear scale with annotations to denote the three tonal sources. The red-thick straight arrows are pointing to the frequency fundamental of 1.9 Hz, which corresponds to the turbine blade passage frequency and higher harmonics.

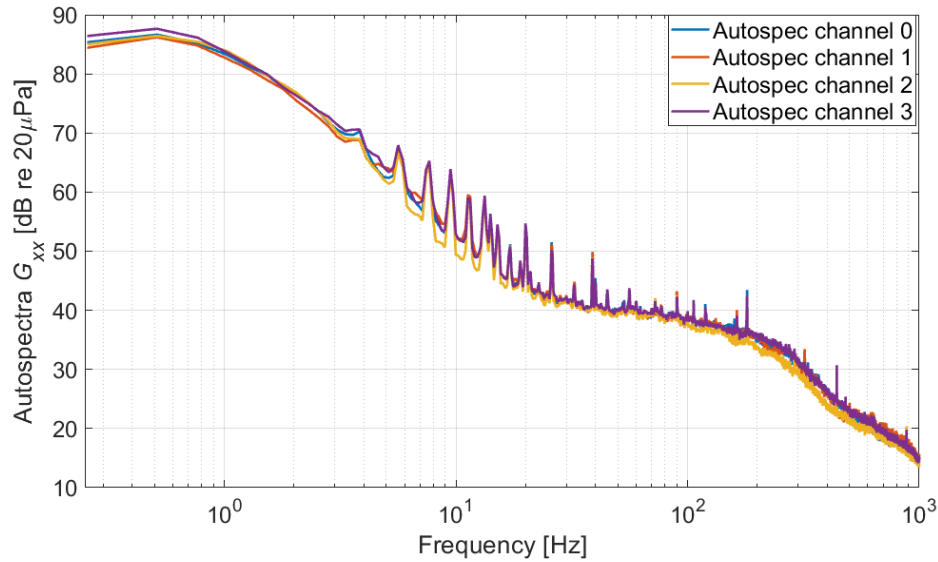


**Figure 9.** Wind turbine noise autospectra at the probe microphones.

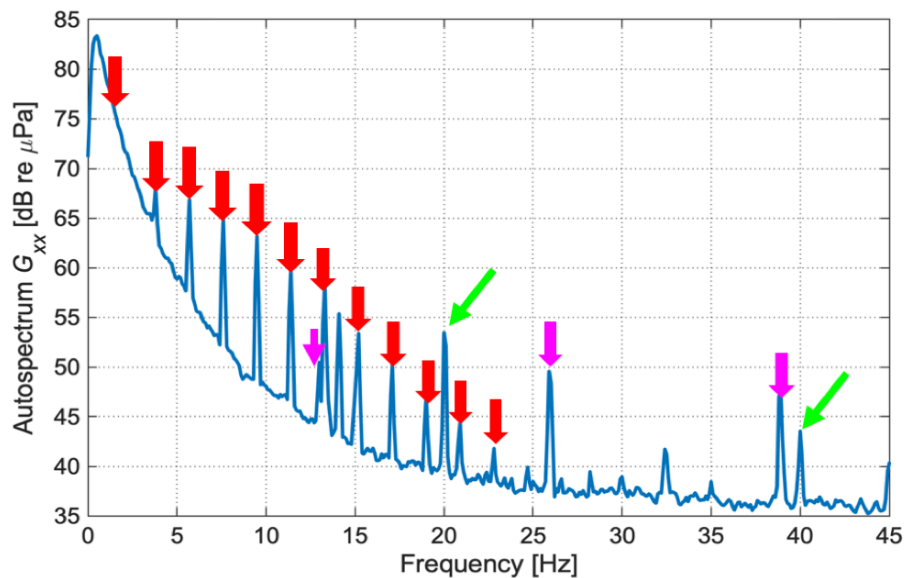


**Figure 10.** Wind turbine noise autospectrum from 0 – 45 Hz.

It is noted again that the hardware and probe configuration was different than for the previously described rocket experiment. In particular, the microphones had an improved low-frequency response, but unknown phase matching, and significantly greater spacing. This microphone separation distance is beneficial in that it may help overcome low-frequency microphone mismatch (thereby improving low-frequency results). The greater spacing also results in lower coherence between channels, which is shown in Figure 11. This low broadband coherence (dominated by wind noise) precludes performing the same type of broadband analysis performed for the rocket noise measurement. Thus, the focus here is the directionality of the tonal components from Figure 10.

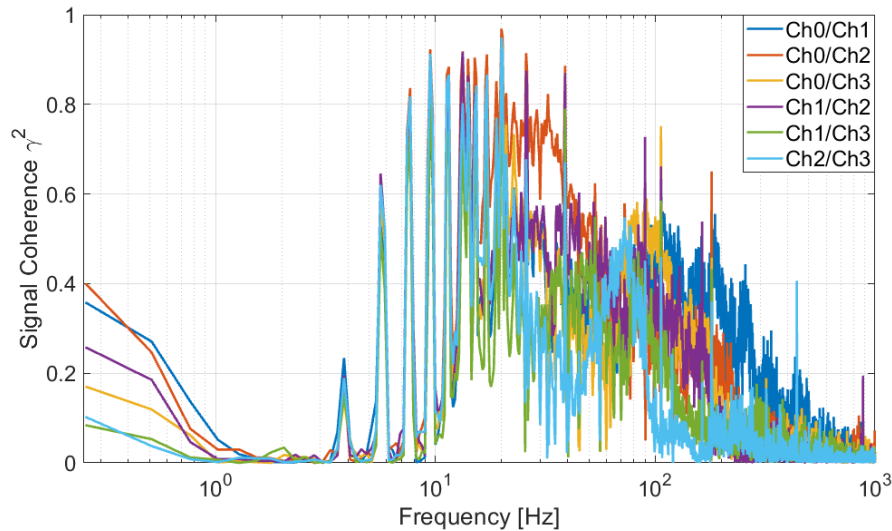


**Figure 11. Wind turbine recording coherence.**

The PAGE-calculated acoustic intensity directions for the highlighted peaks in Figure 10 are shown in Figure 12. The results for the different harmonic series bear out their separation into three sources, with the intensity from the turbine blade passage pointing nominally around  $0^\circ$ , which is similar to “tonal source 2.” (Whether this tonal source is a different noise source related to the wind turbine, or not, is unknown.) Considering the probe location and orientation, it can be inferred that “tonal source 1” is very likely the gravel mining operation located approximately  $90^\circ$  relative to the probe main axis. We believe it to be caused by the periodic metallic “clanking” noise of the conveyer belt but this needs further investigation.

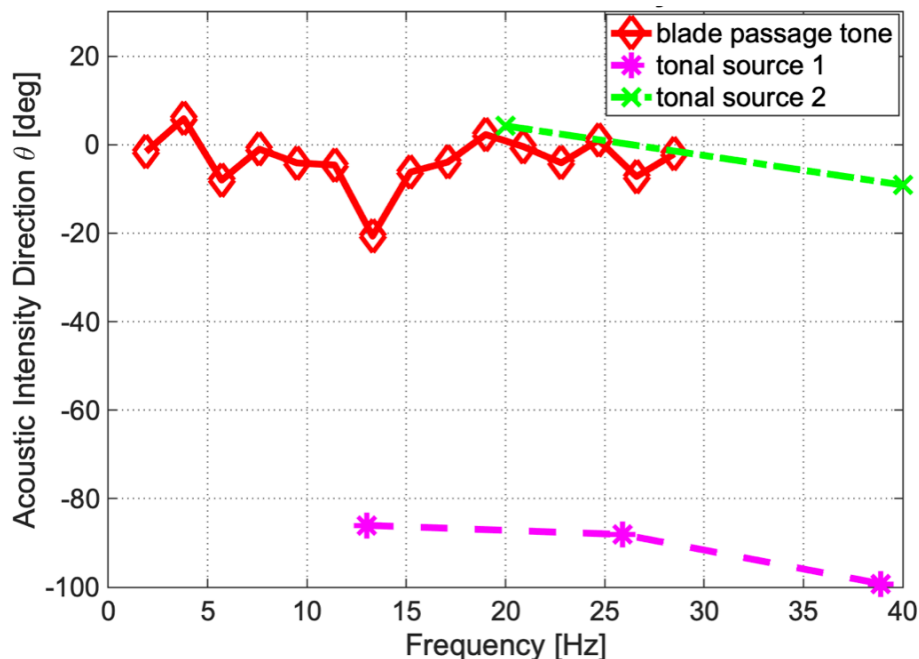


**Figure 12. Acoustic direction calculations for the wind turbine.**

The results for the intensity direction corresponding to the blade passage are within  $\pm 7^\circ$ , with the exception of the 13.3 Hz harmonic. The proximity of this tone to the 13.1 Hz peak coming from the mining operation would interfere and cause an overlap in phase. Note that the 13.3 Hz has the smallest (most negative) phase of any of the harmonics, whereas the 13.1 Hz peak from the mining has the largest (most positive) angle of its three

components. Also, note that in Figure 10, the autospectral component corresponding to the blade passage fundamental (1.9 Hz) appears to be completely masked by wind, but the acoustic intensity direction estimated by the PAGE method (using the pairwise transfer functions between microphones) is in the same direction as the other harmonics. This may be a coincidence, but the ability to estimate intensity direction in situations of poor coherence is under additional investigation.

## 4. CONCLUSION

The present work has shown the successful application of the PAGE intensity method in the upper infrasound and low audio range to the localization of outdoor sources with fairly well-known directions. The bandwidth limitations imposed by the traditional method are addressed by using a larger separation distance for the microphones in the intensity probe, but which is still relatively compact compared to typical infrasound arrays. The limitations of both experiments are noted, as contamination from reflections (rocket test) and other noise sources (wind turbine test) caused some intensity direction errors. Future work will focus on microphone phase calibration at infrasonic frequencies and making measurements for other source fields. Different probe geometries will also be investigated.

## ACKNOWLEDGMENTS

The support of the National Science Foundation is gratefully acknowledged.

## REFERENCES

- <sup>1</sup> F. J. Fahy, "Measurements of acoustic intensity using the cross-spectral density of two microphone signals," *J. Acoust. Soc. Am.* **62**, 1057-1059 (1977).
- <sup>2</sup> F. Jacobsen and H. E. De Bree, "A comparison of two different sound intensity measurements principles," *J. Acoust. Soc. Am.* **118**, 1510-1517 (2015).
- <sup>3</sup> W. F. Druyvesteyn and H. E. De Bree, "A novel sound intensity probe comparison with the pair of pressure microphones intensity probe," *J. Audio Eng. Soc.* **48**, 49-56 (2000).
- <sup>4</sup> J. H. Giraud, K. L. Gee, and J. E. Ellsworth, "Acoustic temperature measurement in a rocket noise field," *J. Acoust. Soc. Am.* **127**, EL 179-EL 184 (2010).
- <sup>5</sup> J. K. Thomson and D. R. Tree, "Finite-difference approximation errors in acoustics intensity measurements," *J. Sound Vib.* **75**, 229-238 (1981).
- <sup>6</sup> E. B. Whiting, J. S. Lawrence, K. L. Gee, T. B. Neilsen and S. D. Sommerfeldt, "Bias errors analysis for phase and amplitude gradient estimation of acoustic intensity and specific acoustic impedance," *J. Acoust. Soc. Am.* **142**, 2208-2018 (2017).
- <sup>7</sup> D. C. Thomas, B. Y. Christensen and K. L. Gee, "Phase and amplitude gradient method for the estimation of acoustic vector quantities," *J. Acoust. Soc. Am.* **137**, 3366-3376 (2015).
- <sup>8</sup> K. L. Gee, T. B. Neilsen, E. B. Whiting, D. K. Torrie, M. Akamine, K. Okamoto, S. Teramoto, and S. Tsutsumi, "Application of a phase and amplitude gradient estimator to intensity-based laboratory-scale jet noise source characterization," Sixth Berlin beamforming conference 2016.
- <sup>9</sup> D. K. Torrie, E. B. Whiting, K. L. Gee, T. B. Neilsen, and S. D. Sommerfeldt, "Initial laboratory experiments to validate a phase and amplitude estimator method for calculation of acoustic intensity," *Proc. Mtgs. Acoust.* **23**, 030005 (2015).
- <sup>10</sup> K. F. Succo, S. D. Sommerfeldt, K. L. Gee, and T. B. Neilsen, "Acoustic intensity of narrowband sources using the phase and amplitude estimator method," *Proc. Mtgs. Acoust.* **30**, 030015 (2017).
- <sup>11</sup> K. L. Gee, T. B. Neilsen, S. D. Sommerfeldt, M. Akamine, and K. Okamoto, "Experimental validation of acoustic intensity bandwidth extension by phase unwrapping," *J. Acoust. Soc. Am.* **141**, EL 357-EL 362 (2017).
- <sup>12</sup> J. Marty, "The IMS infrasound network: current status and technological development". In *infrasound monitoring for atmospheric studies* (pp. 3-62). Springer, cham.

---

<sup>13</sup> K. L. Gee, E. B. Whiting, T. B. Neilsen, M. M. James, and A. R Salton, “Development of a near-field intensity measurement capability for static rocket firings,” *Trans. JSASS Aerospace tech. Japan*. Vol. **14**, no. ISTS30, pp. PO\_2\_9-PO\_2\_15 (2016).

<sup>14</sup> K. L. Gee, F. J. Irarrazabal, M. R. Cook, S. D. Sommerfeldt, T. B. Neilsen, M. C. Mortensen, and Pauline Nelson, “Overview of the phase and amplitude gradient estimator method for the acoustic intensity,” *Internoise Madrid 2019*.